470 J. Chem. Eng. Data **1994,** *39,* 470–474

An Apparatus and Procedure for Measuring Mutual Solubilities of Hydrocarbons + Water: Benzene + Water from 303 to 373 K

Huaping Chen and Jan Wagner*

School of Chemical Engineering, Oklahoma State University, Stillwater, Oklahoma 74078

A continuous-flow-type liquid–liquid equilibrium apparatus has been designed, constructed, and used to measure the mutual solubilities of hydrocarbon + water systems. New results for benzene + water have been determined in the temperature range of 303–373 K at pressures within 1 bar of the three-phase curve. The results compare favorably with the literature values in the 303–333 K temperature range. The solubility of benzene in water matches the lower range of the high-temperature data (373–473 K). The relative errors in both liquid-phase compositions are less than 6% for all values. For benzene + water, the mutual solubility is correlated and used to estimate enthalpies of solution of benzene in water and water in benzene; results are in good agreement with literature values based on calorimetric measurements.

Increasingly stringent emission standards are forcing many refineries and petrochemical plants to modify or totally replace waste water treatment systems (*1*). While solvent extraction has been recognized as one of the best developed available technologies for refinery waste water treatment, reliable liquid–liquid equilibrium data needed for the design of extraction processes are not plentiful. The very low liquid–liquid mutual solubilities of water and hydrocarbons pose significant difficulties in performing accurate and reliable measurements (*2*). Large variations, and even conflicts, are common in the values reported in the temperature range of 303–373 K. To resolve conflicts in the liquid–liquid mutual solubility data for hydrocarbon + water mixtures in this temperature range and to obtain reliable new measurements, we constructed and operated a liquid–liquid equilibrium apparatus. The flow-through unit facilitates sampling equilibrium phases and subsequent sample treatment and analysis.

We began our measurements with the benzene + water binary system because it has been extensively studied (*3*) and could serve as a basis for testing the performance of both the equilibrium unit and overall experimental procedures. In addition, this system is of immediate practical concern with the promulgation of the National Emission Standards for Hazardous Air Pollutants; Benzene (*4*).

Experimental Section

Two key points had to be addressed to successfully design and operate a continuous-flow-type equilibrium unit to obtain equilibrium mutual solubilities for water + hydrocarbon systems. First, mass transfer between the two liquid phases must be accomplished well before the two phases are separated at equilibrium. Second, the two phases must be completely separated after equilibrium is reached. The physical properties of the aqueous systems considered are different from most of the previous vapor–liquid or liquid–liquid equilibrium systems which have been experimentally studied using flow-type equilibrium cells (*5–7*). The liquid water and liquid hydrocarbon mixtures have very high interfacial tensions in the temperature range studied. This results in a high mass transfer resistance between the two phases. Meanwhile, the tendency to form emulsions prohibits the vigorous mixing of the two phases. The design of the experimental apparatus must provide mixing at a level to promote mass transfer while avoiding the formation of emulsions which hinders subsequent phase separation.

In vapor–liquid equilibrium measurements using a flow-through-type equilibrium unit, a large range of flow rates may have a relatively small effect on the phase separation. However, the situation is entirely different when liquid–liquid equilibrium measurements are being made. At the low concentrations of solute addressed in this work, the entrainment of a small droplet of one phase into another phase due to variation in flow rates can lead to very large errors. Therefore, relatively low flow rates are preferred to assure complete separation of the two liquid phases inside an equilibrium cell and to minimize possible liquid entrainment.

A schematic diagram of the experimental apparatus is shown in Figure 1 and is similar to systems described by Thies and Paulatis (*5*) and Wang and Chao (*6*). A flow system is used to mix and, subsequently, to separate and sample the two liquid phases. An LDC Analytical Type NSI-33R minipump with a flow rate range of 46–460 $cm^3 \cdot h^{-1}$ is used to feed water and hydrocarbon continuously to the equilibrium unit. Approximately 4.8 m of 0.635-cm-o.d. stainless steel tubing is used to promote the mixing of the hydrocarbon and water phases. The first 1.2 m of tubing is fitted with a static mixer made from a band of notched and twisted stainless steel sheet metal. The remaining 3.6 m of tubing is packed with approximately 1.5-mm-diameter glass beads. A heating tape is wrapped around the last 1.2 m of tubing to provide optional preheating of the feed.

The liquid mixture from the mixing line enters a 10-m × 0.32-cm-o.d. stainless steel tube. This coiled tube is immersed in a constant-temperature bath and used to bring the feed mixture to equilibrium before it enters the equilibrium cell. The 3.6-m × 0.635-cm-o.d. tubing used by Wang and Chao (*6*) does not provide enough residence time to accomplish the mass transfer for the systems we have studied. The 30-m × 0.019-cm-i.d. tubing used as a preheater by Christensen (*7*) is not adequate because the interfacial area for mass transfer is too small for the mixture to reach equilibrium.

The two equilibrated liquids are separated inside a modified Jerguson JT-40 sight gauge. The total internal volume of the cell is about 60 mL. The sight gauge was modified by tapping a port for the feed and replacing the inside fiber gaskets with two layers of Union Carbide Grafoil graphite tape. Spring washers were installed to accommodate thermal expansion. The less-dense hydrocarbon phase exits from the top of the cell, and the more-dense water phase exits from the bottom.

The equilibrium cell and preheat coil are immersed in a Neslab TEV 70 constant-temperature bath filled with Dow-

0021-9568/94/1739-0470$04.50/0

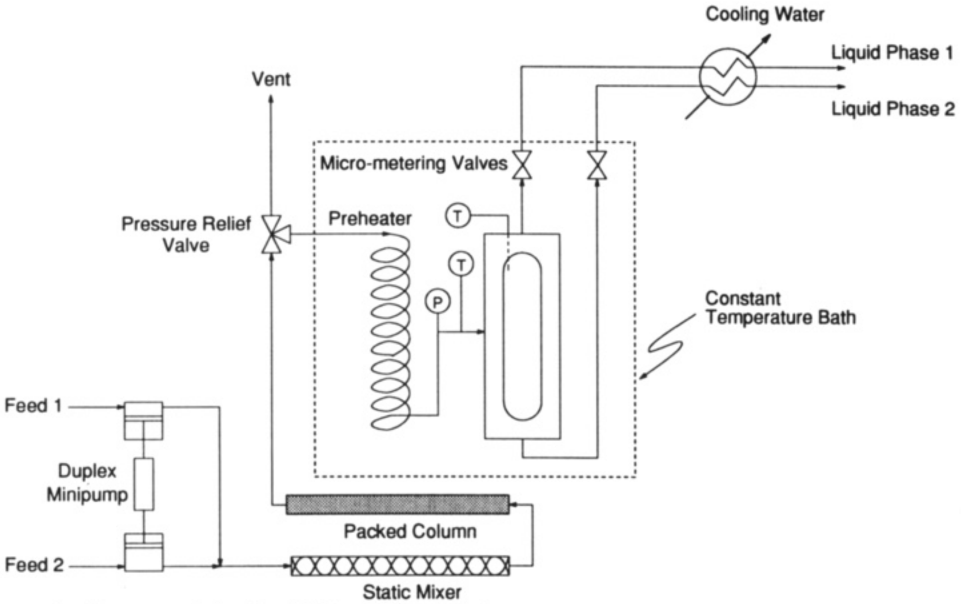

Figure 1. Schematic diagram of the liquid–liquid equilibrium apparatus.

Corning Silicon 200 heat transfer fluid. The bath temperature is measured with an iron–constantan thermocouple calibrated against a laboratory platinum resistance thermometer that is NBS traceable. The uniformity of the bath temperature is better than 0.1 K. The bath temperature is controlled within ±0.2 K of the set point. The temperature inside the cell is also monitored, and the difference between the cell temperature and bath temperature is less than 0.1 K. A Sensotec STJE-AP112 pressure transducer and 450D readout device are used to measure the cell pressure at the feed port of the cell.

During the evaluation of the equilibrium apparatus, we found that the dead volume between the cell outlet and the sampling port must be minimized. The temperature and pressure in the sampling ports are lower than those in the equilibrium cell, resulting in the possibility of phase separation. If this occurs, droplets of the dispersed liquid phase can accumulate on the walls of tubing or in dead volumes (such as the internal volume under the diaphragms of the back-pressure regulators or valve bodies). The accumulated fluid periodically reenters the flow stream and, thus, causes large concentration fluctuations in the collected samples. To minimize the dead volume, a back-pressure regulator is not used. Instead, the pressure control is accomplished by manually adjusting the two Whitey Series SS-22RS2 micrometering valves. These valves, together with the equilibrium cell and the preheat coil, are immersed in the constant-temperature bath to minimize the potential for phase separations in the valve bodies. Capillary bore stainless steel tubing leads from the regulating valves through a water-cooled heat exchanger to the sampling ports. No significant variations in the phase compositions are observed when the combined (total) flow rate is less the 4 cm^3·min^{-1} and the volumetric feed ratio of hydrocarbon to water is between 0.5 and 2.

Sampling Procedure. Proper sampling procedures are extremely important for accurate determination of the mutual solubilities of water + hydrocarbon systems. In the 100–1000 ppm (by weight) concentration range, a slight evaporation of the hydrocarbon component from the aqueous phase can greatly affect the results; the measured hydrocarbon solubility tends to be lower than the true value. For water dissolved in the hydrocarbon phase, the situation is even more complicated. Water can evaporate from the sample, or water can be absorbed into the sample, depending on the humidity of the environment where the sample is taken. Thus, the sampling process must be conducted to minimize exposure to the atmosphere. The following sampling procedure has been adopted.

Table 1. Gas Chromatograph Operating Conditions

operating condition	hydrocarbon-phase analysis	water-phase analysis
injector temperature, °C	240	200
column temperature, °C	240	200
detector temperature, °C	240	220
carrier/reference gas flow, cm^3·min^{-1}	30	30
auxiliary gas flow, cm^3·min^{-1}	40	40

All samples are collected consecutively from the cell at time intervals corresponding to half the residence time of the organic phase in the cell. A 25 or 60 cm^3 sampling vial is filled with 0.5–4.0 cm^3 of dehydrated ethanol solvent depending on the concentration of the sample being collected. The vial is then closed by a screw-cap fitted with a Teflon-coated septum. The capillary tubing from the equilibrium cell passes through the septum and ends beneath the surface of the ethanol. Upon exiting the equilibrium cell, the stream to be sampled is cooled, at which point it forms a two-phase emulsion before entering the sample vial, where it is blanketed by the ethanol solvent to minimize sample loss. The septum used to cap the vial prevents any contact with the atmosphere. At the completion of sampling, the vial is carefully removed from the sampling port *without being mixed*, capped, and stored at 277 K. Prior to GC analysis, the vial is shaken to provide a single-phase mixture of the sample and ethanol; 2 μL of this mixture is then injected into the GC, avoiding any contact with the atmosphere.

Gas Chromatographic Analysis. A Hewlett-Packard 5880A gas chromatograph equipped with a thermal conductivity detector (TCD) is used for both water- and hydrocarbon-phase analyses. A 2.4-m × 0.318-cm Porapak Q column from Alltech is used. Chromatographic grade helium is used as the carrier gas. The operating conditions for the hydrocarbon- and water-phase analyses are shown in Table 1. The analytical procedure used in the sample treatment and analyses is outlined here. Details are described by Chen and Wagner (*8*).

Hydrocarbon solubility in water is characterized by a minimum at approximately room temperature. Direct preparation of single-phase liquid mixtures for use as GC standards

Table 2. Mutual Solubilities of Benzene + Water[a]

		benzene solubility in water			water solubility in benzene		
T, K	P, bar	10^3x	$10^3\sigma(x)$	N	10^3x	$10^3\sigma(x)$	N
303.15	1.0	0.424	0.0231	6	3.84	0.173	6
313.15	1.0	0.464	0.0231	6	4.74	0.217	6
323.15	1.0	0.510	0.0369	6	7.23	0.563	6
333.15	1.5	0.565	0.0346	6	9.5	0.260	6
343.15	2.5	0.625	0.0369	10	12.2	0.260	10
353.15	2.5	0.699	0.0185	6	15.4	0.390	6
363.15	3.5	0.800	0.0323	14	20.7	0.390	14
373.15	3.5	0.950	0.0254	10	26.5	0.303	10

[a] x = mole fraction, $\sigma(x)$ = standard deviation, and N = number of measurements.

with compositions comparable to those encountered at higher temperatures is not feasible. Use of single-phase vapor mixtures as GC standards can resolve this difficulty (*9*), but the results may be subject to large errors due to the technical difficulties involved. Using a cosolvent can resolve the low-temperature immisibility problem. However, it is difficult to control the composition of standards to give calibration points evenly distributed over the composition range of interest. More seriously, such a procedure does not give a clear indication of the approach to the nonlinear response region of the GC. This, in turn, makes it very difficult to treat either the calibration data or sample analysis data correctly.

To resolve the low-temperature immisibility problem, we developed a very simple procedure. For benzene + water, we prepare two calibration curves to measure water solubility in benzene and benzene solubility in water: water + ethanol and benzene + ethanol.

All calibration standards are prepared gravimetrically, and all calibration curves are regressed as log(mass ratio) as a function of log(area ratio). This calibration method is both simple and straightforward. More importantly, it significantly reduces the magnitude of uncertainties and errors in the calibrations from approximately 10% or greater (which is very common for these highly dilute systems) to less than 1%.

Sample analysis for water solubility in the organic phase must include a correction for the water introduced by the ethanol solvent. An ethanol solvent blank is analyzed, and the water content of the ethanol solvent is obtained. This result is then used to correct the GC analysis of the hydrocarbon-phase sample. This correction is discussed elsewhere by Chen and Wagner (*8*).

Materials. Spectral grade benzene with a purity of 99+ mol % from Aldrich Chemical Co. and distilled/deionized water were used without further purification. Ethanol, USP Absolute-200 Proof from AAPER Alcohol and Chemical Co., was dehydrated and stored over 4A molecular sieves from Fisher Scientific Co.

Results and Discussion

Mutual solubilities for benzene + water presented in Table 2 consist of the average of at least six replicate determinations. From these extensive replications, we estimate the maximum relative error for any reported value is less than 6%. The maximum correction for water content introduced by the ethanol cosolvent is less than 15%. The experimental pressure is also included in Table 2. Since all measurements are made within 1 bar of the three-phase curve, the effect of pressure on liquid–liquid equilibrium can be neglected (*10*).

Benzene Solubility in Water. As shown in Figure 2, our solubilities for benzene in water agree well with values reported by Alexander (*11*), Bradley et al. (*12*), Bittrich et al. (*13*), and Tsonopoulos and Wilson (*14*). The values of Udovenko et al. (*15*) show higher benzene solubilities, while the values of Arnold et al. (*16*), Franks et al. (*17*), and Sanemasa et al. (*18*) are lower. The results of Arnold et al. (*16*) have essentially been reproduced by Franks et al. (*17*). The close agreement between these two sets of measurements may result from both groups using similar experimental apparatus, procedure, analytical techniques, and calibration methods.

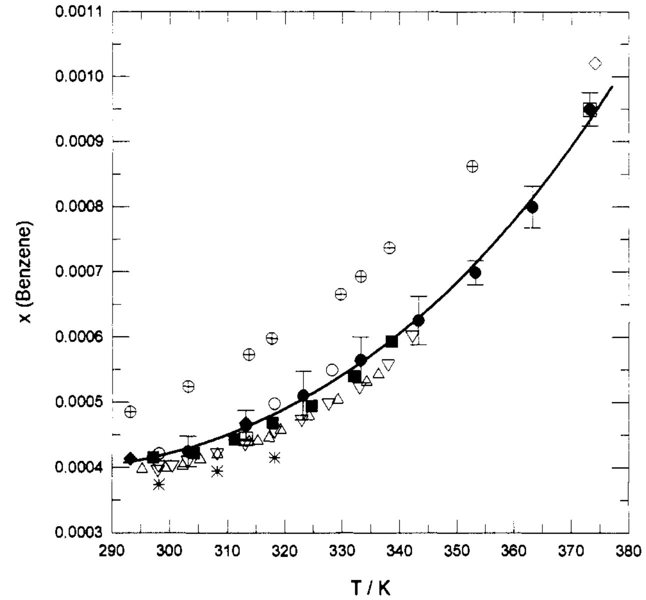

Figure 2. Solubility of benzene in water: (●) this work, (■) Alexander (*11*), (◇) Anderson and Prausnitz (*9*), (▽) Arnold et al. (*16*), (♦) Bittrich et al. (*13*), (○) Bradley et al. (*12*), (△) Franks et al. (*17*), (*) Sanemasa et al. (*18*), (□) Tsonopoulos and Wilson (*14*), (⊕) Udovenko and Aleksandrova (*15*).

The new measurements in the temperature range from 335 to 375 K bridge a gap in the previous benzene solubility measurements and tie the published low-temperature data (less than 340 K) to high-temperature (373–540 K) data. Our measurements at 373.15 K agree very well with the benzene solubilities reported for the lower range of the high-temperature values, as exemplified by the solubilities reported by Tsonopoulos and Wilson (*14*) at 373 K and Anderson and Prausnitz (*9*) at 374 K.

Benson and Krause (*19*) and Wilhelm et al. (*20*) have discussed the merits of different forms of empirical equations for correlating the temperature dependence of high-precision solubility data. We have used the following empirical relation for benzene solubility:

$$\ln\frac{1}{x_b} = -6.191 + 14.03\frac{1}{T_{rb}} - 3.511\frac{1}{T_{rb}^{2}} \qquad (1)$$

where x_b is the mole fraction of benzene and T_{rb} is the system temperature divided by the critical temperature of benzene, 562.2 K. The constants in eq 1 are obtained by least-squares regression procedures. This relationship is shown as the solid line in Figure 2. From the Gibbs–Duhem equation, assuming the activity coefficients for both water in the water phase and for the hydrocarbon in the hydrocarbon phase are equal to 1, we have

$$\left(\frac{\partial \ln x_i}{\partial T}\right)_P \cong \frac{\Delta H_i}{RT^2} \qquad (2)$$

where the heat of solution, ΔH_i is the difference between the partial molar enthalpy of component i in solution, H_i, and

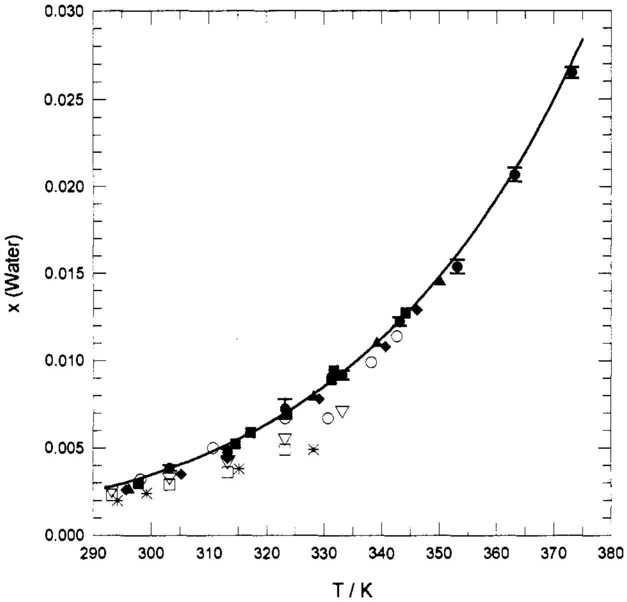

Figure 3. Solubility of water in benzene (literature data before 1950): (●) this work, (□) Berkengeim (*24*), (∗) Clifford (*25*), (▲) von Groschuff (*30*), (○) Hill (*28*), (▽) Rosenbaum and Walton (*26*), (■) Staveley et al. (*31*), (♦) Tarassenkow and Poloshinzewa (*35*).

the pure molar enthalpy, H_i°, at temperature T:

$$\Delta H_i = H_i - H_i^\circ \qquad (3)$$

The partial molar heat capacity at constant pressure, ΔC_{Pi}, is defined by

$$(\partial(\Delta H_i)/\partial T)_P = \Delta C_{Pi} \qquad (4)$$

where

$$\Delta C_{Pi} = C_{Pi} - C_{Pi}^\circ \qquad (5)$$

and C_{Pi}° is the specific heat of the pure component at temperature T. Using eqs 1, 2, and 4, ΔH_i and ΔC_{Pi} at 298.15 K are estimated as 3.69 kJ·mol^{-1} and 208 J·mol^{-1}·K^{-1}, respectively. The estimated heat capacity compares well with the calorimetrically measured value of 225 J·mol^{-1}·K^{-1} reported by Gill et al. (*22, 23*).

The temperature at which benzene reaches its minimum solubility in water is estimated from eq 1 as 281 K; Gill et al. (*22, 23*) report a value of 288.9 K from calorimetric measurements.

Water Solubility in Benzene. There are many published measurements for this system, and the agreement among these data is fair. From Figures 3 and 4, water solubilities measured by Berkengeim (*24*), Clifford (*25*), Rosenbaum and Walton (*26*), Bittrich et al. (*13*), and Englin et al. (*27*) are generally low. The data by Hill (*28*) show a weaker temperature dependence of solubility than the majority of other data. Tsonopoulos and Wilson (*14*) state that their "...new measurements at 373 K are unaccountably too low". Water solubilities measured by Anderson and Prausnitz (*9*) are also low at 373 K. Nevertheless, considering the experimental difficulty and uncertainty involved in measuring the water solubility data, our new measurements are in excellent agreement with the majority of the literature data, especially those of Moule and Thurston (*29*), von Groschuff (*30*), Staveley (*31, 32*), Goldman (*33*), Karlsson (*34*), and Tarassenkow and Poloshinzewa (*35*) in both the trend and absolute values.

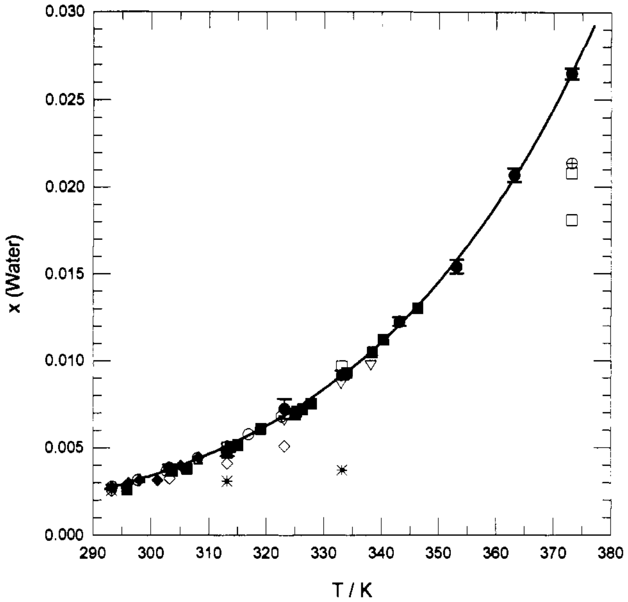

Figure 4. Solubility of water in benzene (literature data after 1950): (●) this work, (⊕) Anderson and Prausnitz (*9*), (∗) Bittrich et al. (*13*), (◇) Englin et al. (*27*), (△) Goldman (*33*), (♦) Karisson (*34*), (○) Moule and Thurston (*29*), (▽) Pavia (*37*), (■) Staveley et al. (*32*), (□) Tsonopoulos and Wilson (*14*).

The water solubility data in Table 2 can be correlated with the following equation, as shown by the solid lines in Figures 3 and 4:

$$\ln(1/x_w) = -1.557 - 9.415 \ln T_{rw} \qquad (6)$$

where x_w is the mole fraction of water and T_{rw} is the system temperature divided by the critical temperature of water, 647.3 K. The uncertainty in the experimental data indicates this exponential correlation may be adequate, as shown in Figures 3 and 4. From eqs 2 and 6, the heat of the solution at 298.15 K is estimated as 23.3 kJ·mol^{-1} from the solubility measurements. The calculated heat of solution is very close to the hydrogen-bonding energy (21–29 kJ·mol^{-1}). This result is in line with current theory and experimental evidence (*36*), which indicates that liquid water dissolving into a nonpolar hydrocarbon liquid phase is virtually a process of breaking hydrogen bonds. The specific heat of mixing at 298.15 K is estimated as 78.3 J·mol^{-1}·K^{-1} from eq 6.

Summary and Conclusions

A continuous-flow-type liquid–liquid equilibrium unit has been designed, constructed, and evaluated. The unit was tested thoroughly using the benzene + water binary. A relatively simple gas chromatographic method has been developed which permits both water-phase and hydrocarbon-phase samples to be analyzed accurately and efficiently.

New mutual solubility data for benzene + water compare favorably with previously published data and bridge a gap which existed in the temperature range from 333 to 373 K. Estimated heats of solution from solubility measurements of benzene in water agree well with calorimetric measurements. The estimated heat of solution of water in benzene is very close to the hydrogen-bonding energy, which supports the argument that water dissolves into nonpolar organic solvents mainly by breaking hydrogen bonds.

Acknowledgment

Comments and suggestions by Robert L. Robinson, Jr., are acknowledged.

Literature Cited

(1) Norman, M. E.; Kapoor, S.; Smalley, G. A., Jr.; Daniel, B. M. *Oil Gas J.* **1992**, June, 54.

(2) Brady, C. J.; Cunningham, J. R.; Wilson, G. M. *Water-Hydrocarbon Liquid-Liquid-Vapor Equilibrium Measurements to 530 °F*; Gas Processors Association: Tulsa, Oklahoma, 1982; RR-62.

(3) Hefter, G. T. In *IUPAC Solubility Data Series*; Shaw, D. G., Eds.; Pergamon: New York, 1989; Vol. 37, pp 63–85.

(4) *Fed. Regist.* **1990**, *55* (45), 8292.

(5) Thies, M. C.; Paulatis, M. E. *J. Chem. Eng. Data* **1984**, *29*, 438.

(6) Wang, Q.; Chao, K. C. *Fluid Phase Equilib.* **1990**, *59*, 207.

(7) Christensen, S. P. Ph.D. Dissertation, University of Delaware, 1990.

(8) Chen, H.; Wagner, J. *J. Chem. Eng. Data*, following paper in this issue.

(9) Anderson, F. E.; Prausnitz, J. M. *Fluid Phase Equilib.* **1986**, *32*, 63.

(10) Sawamura, S.; Kitamura, K.; Taniguchi, K. *J. Phys. Chem.* **1989**, *93*, 4931.

(11) Alexander, D. M. *J. Phys. Chem.* **1959**, *63*, 1021.

(12) Bradley, R. S.; Dew, M. J.; Munro, D. C. *High Temp.—High Pressures* **1973**, *5*, 169.

(13) Bittrich, H. J.; Gedan, H.; Feix, G. *Z. Phys. Chem. (Leipzig)* **1979**, *260*, 1009.

(14) Tsonopoulos, C.; Wilson, G. M. *AIChE J.* **1983**, *29*, 990.

(15) Udovenko, V. V.; Aleksandrova, L. P. *Zh. Fiz. Khim.* **1963**, *37*, 52.

(16) Arnold, D. S.; Plank, C. A.; Erikson, E. E.; Pike, F. P. *Chem. Eng. Data Ser.* **1958**, *3*, 253.

(17) Franks, F.; Gent, M.; Johnson, H. H. *J. Chem. Soc.* **1963**, 2716.

(18) Sanemasa, I.; Araki, M.; Deguchi, T.; Nagai, H. *Bull. Chem. Soc. Jpn.* **1982**, *55*, 1054.

(19) Benson, B. B.; Krause, D., Jr. *J. Chem. Phys.* **1976**, *64*, 689.

(20) Wilhelm, E.; Batino, R.; Wilcock, R. J. *Chem. Rev.* **1977**, *77*, 219.

(21) Chen, H.; Wagner, J. *J. Chem. Eng. Data*, in press.

(22) Gill, S. J.; Nichols, N. F.; Wadso, I. *J. Chem. Thermodyn.* **1975**, *7*, 175.

(23) Gill, S. J.; Nichols, N. F.; Wadso, I. *J. Chem. Thermodyn.* **1976**, *8*, 445.

(24) Berkengeim, T. I. *Zavod. Lab.* **1941**, *10*, 592.

(25) Clifford, C. W. *J. Ind. Eng. Chem.* **1921**, *13*, 628.

(26) Rosenbaum, S. L.; Walton, J. H. *J. Am. Chem. Soc.* **1930**, *52*, 3568.

(27) Englin, B. A.; Plate, A. F.; Tugolukov, V. M.; Pyranishnikova, M. A. *Khim. Tekhnol. Topl. Masel.* **1965**, *10*, 42.

(28) Hill, A. E. *J. Am. Chem. Soc.* **1923**, *45*, 1143.

(29) Moule, D. C.; Thurston, W. M. *Can. J. Chem.* **1966**, *44*, 1361.

(30) von Groschuff, E. *Z. Elektrochem.* **1911**, *17*, 348.

(31) Staveley, L. A. K.; Jeffes, J. H. E.; Moy, J. A. E. *Trans. Faraday Soc.* **1943**, *39*, 5.

(32) Staveley, L. A. K.; Johns, R. G. S.; Moor, B. C. *J. Chem. Soc.* **1951**, 2516.

(33) Goldman, S. *Can. J. Chem.* **1974**, *52*, 1668.

(34) Karisson, R. *J. Chem. Eng. Data* **1973**, *18*, 290.

(35) Tarassenkow, D. N.; Poloshinzewa, E. N. *Chem. Ber.* **1932**, *65*, 184.

(36) Franks, F. In *Water, a Comprehensive Treatise*; Franks, F., Ed.; Plenum: New York, 1979; Vol. 2.

(37) Pavia, R. A. M. S. Thesis, North Carolina State College, 1958.

Received for review August 17, 1993. Accepted February 15, 1994.[®] This work was supported in part by the Oklahoma Refiners Waste Control Council and the Oklahoma Center for the Advancement of Science and Technology.

[®] Abstract published in *Advance ACS Abstracts*, May 1, 1994.